Article

Coherent bunching of anyons and dissociation in an interference experiment

https://doi.org/10.1038/s41586-025-09143-3

Received: 19 December 2024

Accepted: 13 May 2025

Published online: 25 June 2025

Check for updates

Bikash Ghosh[1], Maria Labendik[1], Vladimir Umansky[1], Moty Heiblum[1]✉ & David F. Mross[2]

Aharonov–Bohm interference of fractional quasiparticles in the quantum Hall effect generally reveals their elementary charge (e^*)[1–15]. Recently, our interferometry experiments with several 'particle states' reported flux periods of $\Delta\Phi = (e/e^*)\Phi_0$ (with Φ_0 the flux quantum) at moderate temperatures[16]. Here we report interference measurements of 'particle–hole conjugated' states at filling factors $\nu = 2/3$, 3/5 and 4/7, which revealed unexpected flux periodicities of $\Delta\Phi = \nu^{-1}\Phi_0$. The measured shot-noise Fano factor (F) of the partitioned quasiparticles in each of the quantum point contacts of the interferometer was $F = \nu$ (ref. 17) rather than that of the elementary charge $F = e^*/e$ (refs. 18,19). These observations indicate that the interference of bunched (clustered) elementary quasiparticles occurred for coherent pairs, triples and quadruplets, respectively. A small metallic gate (top gate), deposited in the centre of the interferometer bulk, formed an antidot (or a dot) when charged, thus introducing local quasiparticles at the perimeter of the (anti)dot. Surprisingly, such charging led to a dissociation of the 'bunched quasiparticles' and, thus, recovered the conventional flux periodicity set by the elementary charge of the quasiparticles. However, the shot-noise Fano factor (of each quantum point contact) consistently remained at $F = \nu$, possibly due to the neutral modes accompanying the conjugated states. The two observations—bunching and debunching (or dissociation)—were not expected by current theories. Similar effects may arise in Jain's 'particle states' (at lower temperatures) and at even denominator fractional quantum Hall states[20].

Interference measurements of quantum particles offer detailed insights into single-particle dynamics and collective behaviour. Such measurements are particularly valuable for emergent exotic particles that form due to strong interactions between electrons in two dimensions and under strong magnetic fields. These particles carry fractional charges, obey anyonic statistics and produce specific macroscopic signatures such as (fractionally) quantized electronic and thermal Hall conductances.

The properties of individual fractional quasiparticles exhibit striking deviations from those of weakly interacting electrons. Experiments have been designed to measure the scattering phase shifts and quantum coherence times[21], test entanglement between pairs of quantum particles[22], and probe the quasiparticle charge[23–25]. The braiding phase has been measured through interference experiments with Fabry–Perot interferometers[1–12] or Mach–Zehnder interferometers[13–15]. Recently, time-braiding was used to measure the anyonic statistical phase through cross-correlation of partitioned quasiparticles[26–29].

In any fractional quantum Hall interferometer, the interference loop is supported by two QPCs, which serves as 'optical beam splitters', and ballistic propagation along edge channels surrounding the bulk. The QPCs inject discrete charge quanta into a particle beam, which carries shot noise characterized by the Fano factor F (refs. 23–25). Only the fractional charges that exist as bulk quasiparticles can tunnel through the QPC opening, while the QPC transmission is high. The smallest fractional value is the elementary quasiparticle charge e^*, which is typically determined by the denominator of the bulk filling factor ν_b. That is, $e^* = e/3$ at fillings $\nu_b = 1/3$ and 2/3, $e^* = e/5$ at $\nu_b = 2/5$ and 3/5, and $e^* = e/7$ at $\nu_b = 3/7$ and 4/7. Notably, the gapless edge or interface modes impose no constraints, and the interference period is independent of their choice[16,30]. If the tunnelling of individual quasiparticles is responsible for the interference and noise, the Aharonov–Bohm flux periodicity is expected to follow the simple rule, $\Delta\Phi = \Phi_0/F$, where $\Delta\Phi$ is the flux periodicity and Φ_0 the flux quantum.

Our measurements were performed with a chiral (optical-like) Mach–Zehnder interferometer (OMZI)[16,31,32] (Fig. 1). Its flexible design, based on co-propagating 'interface modes', is free of the deleterious effects of Coulomb interactions and allows interfacing of different fractional fillings. In this interferometer architecture, two charged external gates define the interfering interface modes: one gate depletes carriers to filling ν_d, whereas the other gate accumulates carriers to filling ν_a. The edge conductances of the two interface modes are set by the differences in the fillings: $\nu_b - \nu_d$ and $\nu_a - \nu_b$. Two QPCs, QPC1 and QPC2 in Fig. 1, partition the co-propagating interface modes to form a closed interference loop. The chirality of the interface modes prohibits back-reflection; consequently, all incoming charge must pass through the interferometer, and the OMZI displays a pristine Aharonov–Bohm interference pattern, known as 'pajama'[16]. To obtain phase slips in the Aharonov–Bohm interference, quasiparticles were introduced into the bulk of the

[1]Braun Center for Sub-Micron Research, Department of Condensed Matter Physics, Weizmann Institute of Science, Rehovot, Israel. [2]Department of Condensed Matter Physics, Weizmann Institute of Science, Rehovot, Israel. ✉e-mail: moty.heiblum@weizmann.ac.il

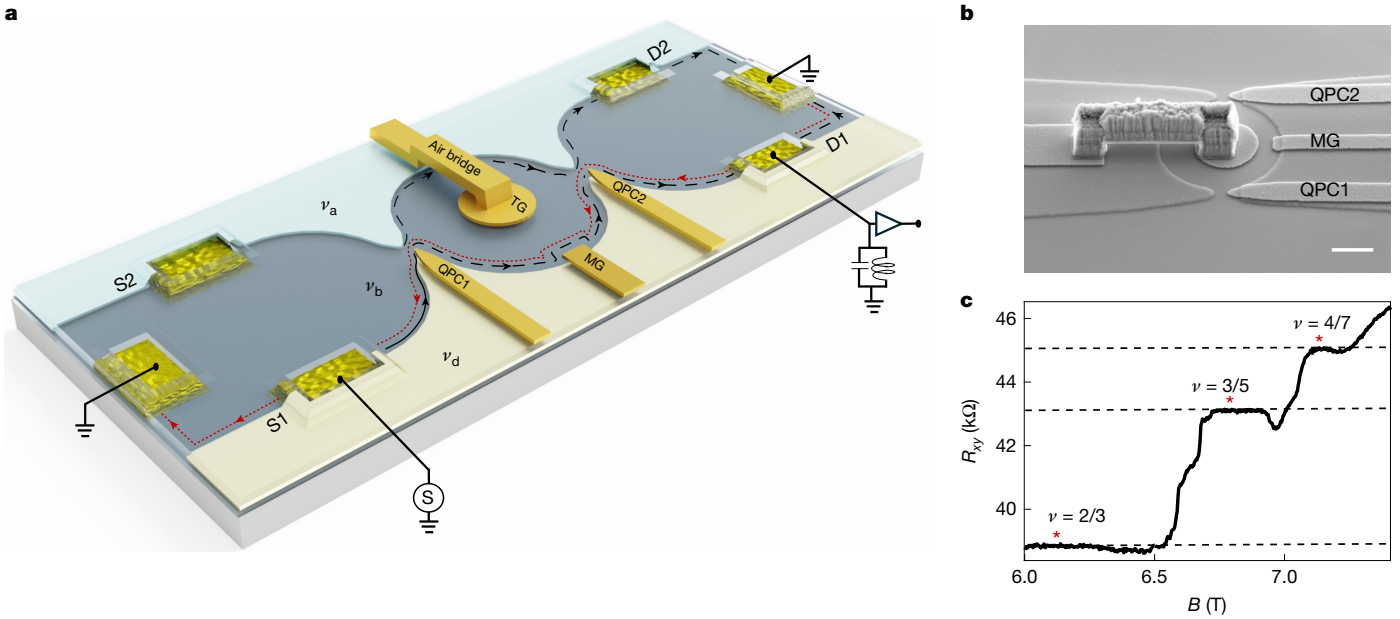

Fig. 1 | Device structure of an OMZI. a, Schematic representation of the OMZI. Its structure has three regions, each tuned to a different filling factor. The central region (the bulk, dark grey) is tuned by the magnetic field B to the filling ν_b. It is flanked by two boundary regions, each tuned to a different filling through the applied voltage to two wide metallic gates. The upper gate (light blue) is positively charged and, thus, accumulates charge, leading to a higher filling, $\nu_a > \nu_b$. The lower gate (light yellow) is negatively charged and, thus, depletes the charge, leading to a lower filling, $\nu_d < \nu_b$. This combination results in two co-propagating interface charge modes with 'effective fillings' $\nu_a - \nu_b$ and $\nu_b - \nu_d$, respectively. This design prevents backscattering of the interface modes and is free of the deleterious effects of the Coulomb interactions. Current is sourced from contact S1 (or S2) at a frequency of 766 kHz. The current is partitioned at QPC1 into two forward-propagating chiral interface modes (dashed black lines in grey region) partitioned further by QPC2. Upstream neutral modes are shown by the red dotted line. The transmitted current is collected by drains D1 and D2, filtered by an LC circuit (resonance at 766 kHz) and amplified by a cold amplifier. A small metallic top gate was deposited at the centre of the interferometer bulk to induce an antidot (or a dot) that introduces localized quasiparticles at its perimeter. **b**, Scanning electron micrograph of the heart of the interferometer. **c**, Transverse Hall resistance as a function of the magnetic field showing quantized plateaux at the fractional fillings under study. The stars (*) on each plateau indicate the tuned magnetic field B where the interference and shot noise were measured. MG, modulation gate; TG, top gate. Scale bar, 500 nm.

interferometer by charging a small metallic top gate, thus forming an isolated antidot (or a dot) in the centre of the interferometer (Fig. 1)[16]. Our experiments were conducted with two OMZI devices featuring slightly different QPC transmissions. The fabricated internal area of both OMZIs $A = 3\ \mu m^2$, and there was a single path length of 3 µm. The top-gate radii were 0.5 µm (OMZI1) and 0.35 µm (OMZI2).

Previous OMZI studies of three particle-like bulk fillings, $\nu_b = 1/3, 2/5$ and 3/7, found Aharonov–Bohm interference with magnetic flux periodicities $\Delta\Phi \approx (e/e^*)\Phi_0$, which was set by the elementary quasiparticle charges at an electron temperature of 15–20 mK (ref. 16). Additionally, charging the top gate yielded phase slips with the theoretically expected magnitudes. Here we present Aharonov–Bohm interference and noise measurements of particle–hole conjugated bulk fillings $\nu_b = 2/3$, 3/5 and 4/7.

We initially kept the top gate uncharged, $V_{TG} = 0$, and measured the shot noise of a single QPC at all three bulk fillings and for different choices of ν_d and ν_a in OMZI1. We consistently obtained the Fano factor $F = \nu_b$ instead of the conventional $F \approx e^*/e$ (Fig. 2). These measurements agree with earlier studies in conventional QPCs, with both sides depleted, $\nu_d = \nu_a$, for a similar temperature range[17,33]. Next, we partially closed the second QPC to form the OMZI and measured the Aharonov–Bohm interference. The observed magnetic flux periodicity was non-integer in all cases and followed the simple rule $\Delta\Phi = \Phi_0/\nu = \Phi_0/F$ (Fig. 3). The most straightforward interpretation of noise and interference measurements is that bunches of two, three or four elementary quasiparticles tunnelled coherently across the QPCs and interfered (see Supplementary Fig. 6 and the discussion below).

The expected periodicity in the 'modulation-gate' voltage of OMZI1, V_{MG}, can be derived as follows. The flux periodicity revealed by the modulation gate should also be $\Delta\Phi = (1/\nu_b)\Phi_0$. The gate repels the charge $\Delta Q = C \times \Delta V_{MG}$ with the capacitance C assumed to be independent of ν_b, leading to a filling-factor-independent periodicity $\Delta V_{MG}\nu_b B = \Phi_0\Pi$, with $\Pi = ne/C$. We found nearly identical values of ΔV_{MG}(2/3, 3/5, 4/7) = (11.7 mV, 10.3 mV, 9.5 mV) in OMZI1.

Next, we charged the top gate of OMZI1 by $V_{TG} = -100$ mV (forming an antidot) or by $V_{TG} = +50$ mV (dot), anticipating phase slips. Unexpectedly, we found that the Aharonov–Bohm flux periodicity changed to $\Delta\Phi \approx (e/e^*)\Phi_0$ at all the three tested fillings, in a similar fashion to the observed Aharonov–Bohm periodicities of particle-like Jain states[16] (Fig. 4a,c,e). Even more surprisingly, the change in the Aharonov–Bohm periodicity was not reflected in the measured properties of a single QPC, whose transmission and Fano factor were not affected by V_{TG} (Supplementary Fig. 6). In particular, the rule $\Delta\Phi = \Phi_0/F$ was violated in this case. For some parameters, a significantly weaker fast Fourier transform (FFT) component of the bunched periodicity $\Delta\Phi \approx \nu_b^{-1}\Phi_0$ also remained (Fig. 4b,d,f and Supplementary Fig. 9). OMZI2 was tested only at $\nu_b = 2/3$ and 3/5 and exhibited the same behaviour (Supplementary Fig. 11).

The periodicity of the modulation-gate voltage in the regime of dissociated quasiparticles also showed unexpected behaviour. Assuming the same modulation-gate capacitance and replacing ν_b by e^*/e led to $\Delta V_{MG}(e^*/e)B = \Phi_0\Pi$, with $\Pi = ne/C$, the observed periodicities at $V_{TG} \approx -100$ mV where ΔV_{MG}(2/3, 3/5, 4/7) = (21.7 mV, 17.4 mV, 15.5 mV). At $\nu_b = 2/3$, the modulation-gate periodicity doubled, just like the magnetic-field periodicity. However, the behaviour at the other fillings differed significantly. Although this behaviour is not understood, we ruled out the possibility that the top gate influences the capacitance: the residual $\Delta\Phi \approx \nu_b^{-1}\Phi_0$ peaks at $\nu_b = 3/5$ remained at a constant modulation-gate periodicity independent of V_{TG} in both devices.

Finally, we show the systematic dependence of the interference peaks on the top-gate voltage at $\nu_b = 3/5$ measured in OMZI2 and at $\nu_b = 2/3$

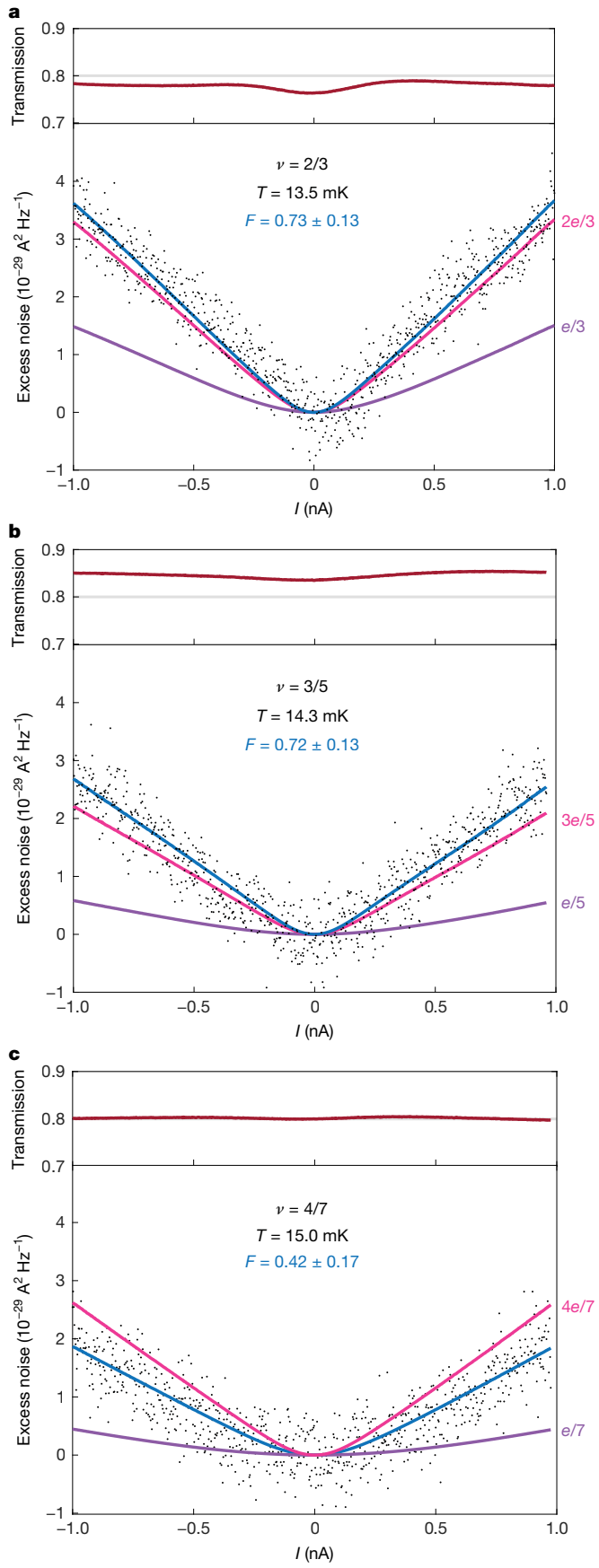

Fig. 2 | Shot noise measured in a single QPC of the OMZI. a–**c**, Noise measured at three particle–hole conjugated states with bulk filling: $\nu = 2/3$ (**a**), $\nu = 3/5$ (**b**) and $\nu = 4/7$ (**c**). Top, nonlinear transmissions of the QPC. Bottom, excess noise as a function of the sourced current. The blue lines represent the fitted curves and the Fano factor F. The pink lines correspond to $F = \nu_b$, and the purple lines correspond to $F = e^*/e$.

in OMZI1. For a sequence of positive top-gate voltages in the range $V_{TG} \approx 0$–70 mV, at $\nu_b = 3/5$, the flux periodicity changed continuously as the quasiparticles dissociated one-by-one with the varying V_{TG} (Fig. 5). It started with the bunched periodicity $\Delta\Phi = (5/3)\Phi_0$ and ended at a dissociated periodicity $\Delta\Phi = 5\Phi_0$ at $V_{TG} = 60$ mV, whereas a weaker bunched periodicity remained. For $V_{TG} > 60$ mV, only the bunched periodicity $\Delta\Phi = (5/3)\Phi_0$ was visible once again.

Our observed bunching should be viewed in the context of earlier shot-noise measurements that found the Fano factor $F = \nu_b$ at low temperatures (approximately 10 mK) and $F = e^*/e$ at higher temperatures[20,33]. In standard QPCs with counter-propagating edges, the low-temperature noise Fano factor follows $F = \nu_b$. Moreover, the same Fano factor was measured on intermediate plateaux in the QPC transmission, where no charge partitioning of the quasiparticles occurred. Consequently, no noise was expected unless it was generated by neutral modes. A specific theoretical model based on stochastic equilibration at the edge was put forth in ref. 30.

The present experiment focused on the low-temperature regime due to vanishing visibility above 60 mK (Supplementary Fig. 10). Intermediate transmission plateaux were not observed in the QPCs of the OMZI with co-propagating edge modes; thus, the contribution of the neutral modes was not established. Moreover, the agreement between the Fano factor and Aharonov–Bohm periodicity through the relation $\Delta\Phi \approx \Phi_0/F$ at $V_{TG} = 0$ strongly indicates an incoherent origin of the increased Fano factor (due to neutral modes). Instead, the combined measurements indicate that coherent bunched quasiparticles, formed by pairs, triplets or quadruples of the elementary quasiparticles, tunnelled at the QPC. Specifically, the measurement reflects a partitioned and interfering quasiparticle charge of $e_\Phi = \nu e$. Note that e_Φ is also the amount of charge that accumulates when one additional flux quantum is threaded in the interferometer. The corresponding quasiparticle is sometimes referred to as a Laughlin quasiparticle (or as a vortex) and is distinct from an elementary quasiparticle with charge e^* (the two coincide for Laughlin states such as $\nu = 1/3$).

Superficially, the observed bunching resembles the pairing and tripling in the integer quantum Hall regime[12,34,35]. Its origin is not well understood, despite theoretical efforts[36]. Several key aspects of the experiments distinguish these observations from the anyon bunching observed here, indicating that they have different origins. Most significantly, the pairing and tripling at integers were only observed when an inner edge mode formed a closed trajectory in the interferometer, and decoherence of the mode destroyed the effect. By contrast, no inner modes were present in the OMZI at zero top-gate voltage.

The most puzzling observation is the dissociation of the interfering quasiparticles upon charging the top gate, indicated by the sudden change in the Aharonov–Bohm flux periodicity. In this case, the Fano factor of the shot noise in each of the QPCs disagreed with the Aharonov–Bohm periodicity, which indicates an incoherent contribution to the shot noise. A consistent physical picture is that, depending on the top gate, either Laughlin quasiparticles or fundamental quasiparticles were partitioned in the QPC. Tunnelling of elementary quasiparticles with charge e^* activated neutral edge modes, which contributed incoherently to the Fano factor, leading to $F = \nu$, but did not change the interference. By contrast, tunnelling of Laughlin quasiparticles did not excite neutral modes at the standard edge with vacuum (Supplementary Section. 12). Moreover, ref. 30 argued that further noise due to neutral modes does not change when edge modes are replaced by interface modes. Consequently, the Fano factor and the Aharonov–Bohm periodicity were both set by the tunnelling charge, $e_\Phi = \nu e$.

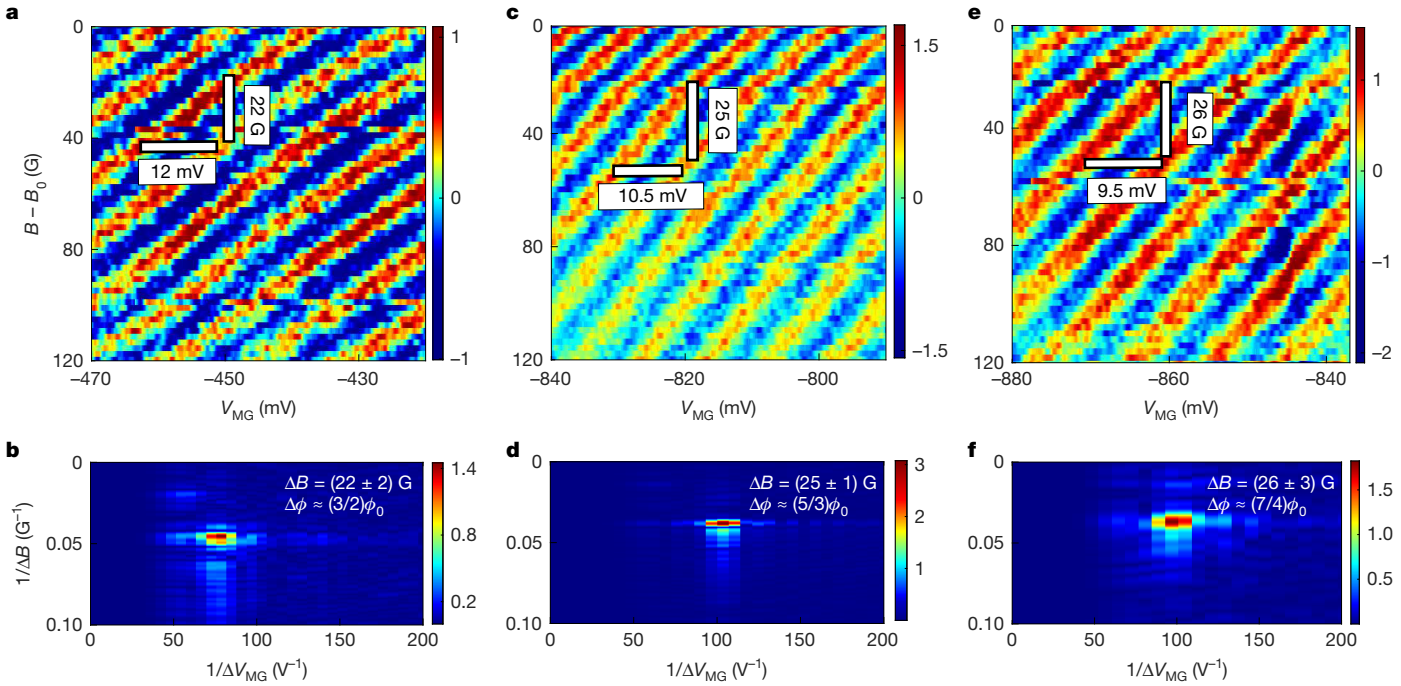

Fig. 3 | Evidence of coherent bunching of anyons in particle–hole conjugated states. a–f, Aharonov–Bohm interference (pajamas) of the measured three states, plotted as a function of magnetic field B and modulation-gate voltage V_{MG}: $\nu_b = 2/3$ (**a**), $\nu_b = 3/5$ (**c**) and $\nu_b = 4/7$ (**e**). Each of the two QPCs is tuned to transmission, $t_1 = t_2 = 0.8$, whereas the top gate is not charged. The corresponding two-dimensional FFTs relate to the states: $\nu_b = 2/3$ (**b**), $\nu_b = 3/5$ (**d**) and $\nu_b = 4/7$ (**f**). The fractional flux periodicities are $\Delta\Phi \approx \nu_b^{-1}\Phi_0$ in all three cases. The depleted and accumulated sides were at $\nu_d = 0$ and $\nu_a = 1$ for all bulk fillings.

Our observations present a new paradigm. At low temperature, the partitioned and interfering quasiparticles were bunched elementary quasiparticles. Moreover, introducing localized quasiparticles by charging the top gate in the interferometer bulk led to phase slips in particle-like states[16]; here, this dissociated the bunched elementary quasiparticles. The mechanism behind these observations remains

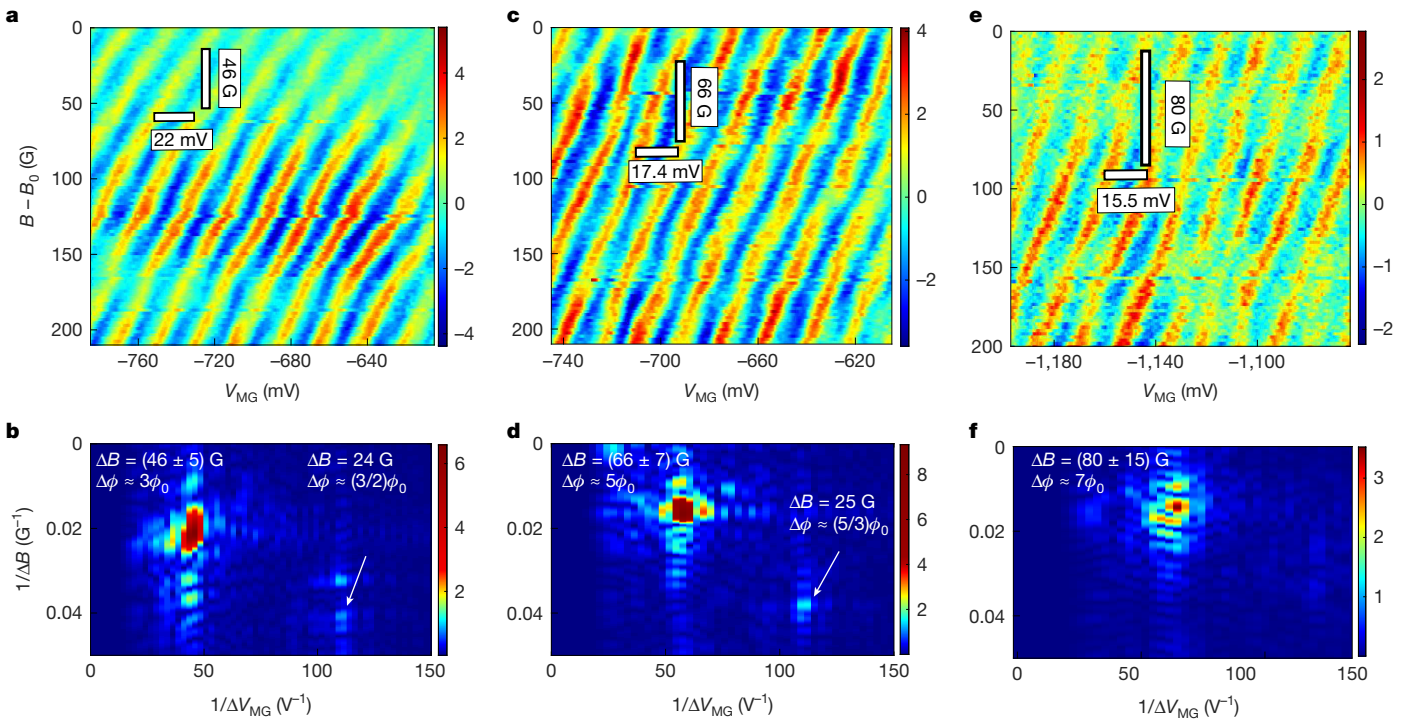

Fig. 4 | Evidence of coherent dissociation of bunched anyons in particle–hole conjugated states. a–f, Activating the top gate with $V_{TG} = -(100–120)$ mV forms an antidot that harbours isolated quasiparticles. An apparent dissociation of the bunched anyons takes place. **a**,**c**,**e**, Typical Aharonov–Bohm pajamas in the B–V_{MG} plane for $\nu_b = 2/3$ (**a**), $\nu_b = 3/5$ (**c**) and $\nu_b = 4/7$ (**e**). The two QPC transmissions ($t_1 = t_2 = 0.8$) were unaffected by V_{TG}. **b**,**d**,**f**, FFTs reflecting the flux periodicities, $\Delta\Phi \approx (e/e^*)\Phi_0$, corresponding to interference of the elementary fractional charges $e/3$ (**b**), $e/5$ (**d**) and $e/7$ (**f**). A weak higher harmonic due to residual bunching is also observable for $\nu_b = 2/3$ and 3/5. However, at filling $\nu_b = 4/7$, the 'bunched periodicity' is absent.

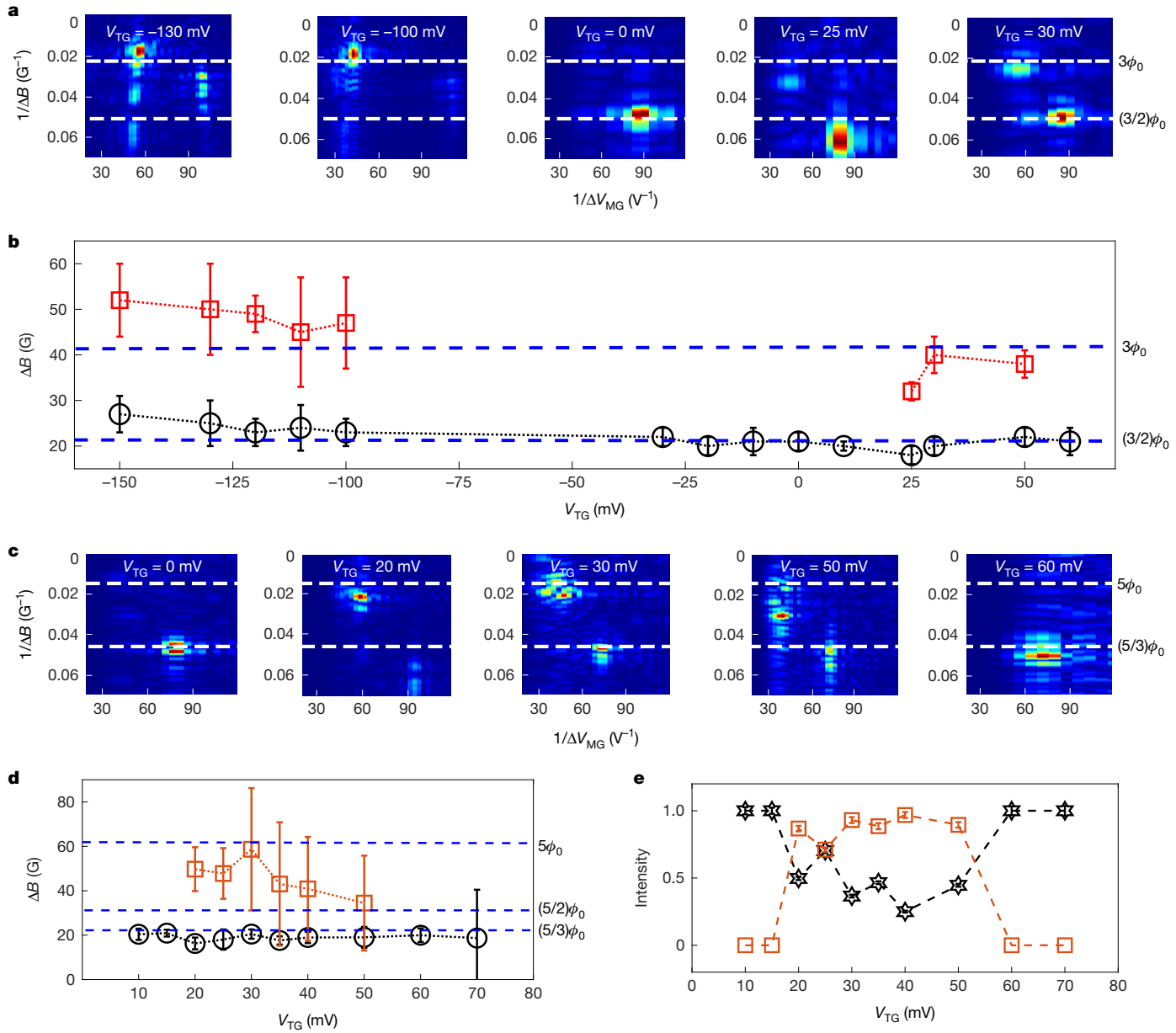

Fig. 5 | Evolution of the dissociated anyons on charging the top gate for $\nu_b = 2/3$ and 3/5. a–**e**, The top gate was incrementally charged within different V_{TG} ranges. For $\nu_b = 2/3$, V_{TG} was varied from −150 to +60 mV, whereas for $\nu_b = 3/5$, V_{TG} was incremented in steps of $\Delta V_{TG} = 5$ mV within the range 0–70 mV. The Aharonov–Bohm pajamas in the B–V_{MG} plane were recorded at each step. **a**,**c**, ΔB peaks are seen in the two-dimensional FFT as a function of V_{TG} for $\nu_b = 2/3$ (**a**) and $\nu_b = 3/5$ (**c**). Anyon dissociation is observed with positive and negative top-gate bias (dot or antidot). **b**, Quasiparticles dissociated in the ranges $V_{TG} = -(150–100)$ mV and $V_{TG} = +25–50$ mV for $\nu_b = 2/3$, showing flux periodicity $\Delta\Phi = 3\Phi_0$. A residual weaker peak remained. The quasiparticles remained fully bunched between −30 and 25 mV with $\Delta\Phi = (3/2)\Phi_0$. We do not have any data from −30 to −100 mV. **d**, For $\nu_b = 3/5$, with V_{TG} below 20 mV or above 50 mV, the quasiparticles remained bunched, with flux periodicity $\Delta\Phi = (5/3)\Phi_0$. An apparent dissociation (red) of the bunched anyons (black) occurred in the range $V_{TG} = (20–50)$ mV, showing partial bunching $\Delta\Phi = (5/2)\Phi_0$ and complete dissociation $\Delta\Phi = 5\Phi_0$ (**c**,**d**). A residual bunched peak remained. The error bars indicate the width of each peak, determined from a Gaussian fit. **e**, Relative weights of the bunched (black) and dissociated (red) FFT peaks as a function of V_{TG} for $\nu_b = 3/5$.

unclear. Localized quasiparticles are expected to produce phase slips in the interference pattern (of bunched or dissociated elementary quasiparticles), but none were observed at any top-gate voltage. A recent Fabry–Perot interferometry experiment in bilayer graphene also reported an absence of phase slips in particle–hole conjugated states, which was attributed to fluctuations in the number of bulk quasiparticles[37]. It is possible that similar fluctuations in the number of quasiparticles under the top gate also cause debunching, which is observed at the same top-gate voltage range where phase slips were observed in particle-like states[16].

Our findings highlight the important of studying particle-like Jain states at very low temperatures where the Fano factor is governed by e_Φ instead of e^* (ref. 20). First, we expect the flux periodicity to change at low temperatures. Second, tracking the previously observed phase slips in the low-temperature regime may provide other vital insights into bunching, dissociation and how they are influenced by adding localized quasiparticles (at will) into the bulk of the interferometer. Control over the interfering quasiparticles will be critical in the search for non-abelian statistics because the Laughlin quasiparticles are abelian even in non-abelian quantum Hall states such as the Moore–Read Pfaffian[38].

Online content

Any methods, additional references, Nature Portfolio reporting summaries, source data, extended data, supplementary information, acknowledgements, peer review information; details of author contributions and competing interests; and statements of data and code availability are available at https://doi.org/10.1038/s41586-025-09143-3.

1. Zhang, Y. M. et al. Distinct signatures for Coulomb blockade and Aharonov-Bohm interference in electronic Fabry-Perot interferometers. *Phys. Rev. B* **79**, 241304 (2009).
2. Ofek, N. et al. Role of interactions in an electronic Fabry–Perot interferometer operating in the quantum Hall effect regime. *Proc. Natl Acad. Sci. USA* **107**, 5276–5281 (2010).
3. Ronen, Y. et al. Aharonov-Bohm effect in graphene-based Fabry-Pérot quantum Hall interferometers. *Nat. Nanotechnol.* **16**, 563–569 (2021).
4. Nakamura, J., Liang, S., Gardner, G. C. & Manfra, M. J. Direct observation of anyonic braiding statistics. *Nat. Phys.* **16**, 931–936 (2020).
5. Kim, J. et al. Aharonov–Bohm interference and statistical phase-jump evolution in fractional quantum Hall states in bilayer graphene. *Nat. Nanotechnol.* **19**, 1619–1626 (2024).
6. Nakamura, J. et al. Aharonov–Bohm interference of fractional quantum Hall edge modes. *Nat. Phys.* **15**, 563–569 (2019).
7. Déprez, C. et al. A tunable Fabry-Pérot quantum Hall interferometer in graphene. *Nat. Nanotechnol.* **16**, 555–562 (2021).
8. Samuelson, N. L. et al. Anyonic statistics and slow quasiparticle dynamics in a graphene fractional quantum Hall interferometer. Preprint at https://arxiv.org/abs/2403.19628 (2024).
9. Werkmeister, T. et al. Anyon braiding and telegraph noise in a graphene interferometer. *Science* **388**, 730–735 (2024).
10. Chamon, C. D. C., Freed, D. E., Kivelson, S. A., Sondhi, S. L. & Wen, X. G. Two point-contact interferometer for quantum Hall systems. *Phys. Rev. B* **55**, 2331–2343 (1997).
11. Willett, R. L. et al. Interference measurements of non-abelian e/4 & abelian e/2 quasiparticle braiding. *Phys. Rev.* **13**, 011028 (2023).
12. Yang, W. et al. Evidence for correlated electron pairs and triplets in quantum Hall interferometers. *Nat. Commun.* **15**, 10064 (2024).
13. Ji, Y. et al. An electronic Mach-Zehnder interferometer. *Nature* **422**, 415–418 (2003).
14. Neder, I., Heiblum, M., Levinson, Y., Mahalu, D. & Umansky, V. Unexpected behavior in a two-path electron interferometer. *Phys. Rev. Lett.* **96**, 016804 (2006).
15. Kundu, H. K., Biswas, S., Ofek, N., Umansky, V. & Heiblum, M. Anyonic interference and braiding phase in a Mach-Zehnder interferometer. *Nat. Phys.* **19**, 515–521 (2023).
16. Ghosh, B. et al. Anyonic braiding in a chiral Mach–Zehnder interferometer. *Nat. Phys.* https://doi.org/10.1038/s41567-025-02960-3 (in the press).
17. Bhattacharyya, R., Banerjee, M., Heiblum, M., Mahalu, D. & Umansky, V. Melting of interference in the fractional quantum Hall effect: appearance of neutral modes. *Phys. Rev. Lett.* **122**, 246801 (2019).
18. de-Picciotto, R. et al. Direct observation of a fractional charge. *Phys. B: Condens. Matter* **249–251**, 395–400 (1998).
19. Reznikov, M., de Picciotto, R., Griffiths, T. G., Heiblum, M. & Umansky, V. Observation of quasiparticles with one-fifth of an electron's charge. *Nature* **399**, 238–241 (1999).
20. Chung, Y. C., Heiblum, M. & Umansky, V. Scattering of bunched fractionally charged quasiparticles. *Phys. Rev. Lett.* **91**, 216804 (2003).
21. Schuster, R. et al. Phase measurement in a quantum dot via a double-slit interference experiment. *Nature* **385**, 417–420 (1997).
22. Neder, I. et al. Interference between two indistinguishable electrons from independent sources. *Nature* **448**, 333–337 (2007).
23. dePicciotto, R. et al. Direct observation of a fractional charge. *Nature* **389**, 162–164 (1997).
24. Saminadayar, L., Glattli, D. C., Jin, Y. & Etienne, B. Observation of the e/3 fractionally charged Laughlin quasiparticle. *Phys. Rev. Lett.* **79**, 2526–2529 (1997).
25. Simmons, J. A. et al. Resistance fluctuations in the integral-quantum-Hall-effect and fractional-quantum-Hall-effect regimes. *Phys. Rev. B* **44**, 12933–12944 (1991).
26. Lee, J.-Y. M. et al. Partitioning of diluted anyons reveals their braiding statistics. *Nature* **617**, 277–281 (2023).
27. Glidic, P. et al. Cross-correlation investigation of anyon statistics in the v=1/3 and 2/5 fractional quantum Hall states. *Phys. Rev.* **13**, 011030 (2023).
28. Ruelle, M. et al. Comparing fractional quantum Hall Laughlin and Jain topological orders with the anyon collider. *Phys. Rev.* **13**, 011031 (2023).
29. Bartolomei, H. et al. Fractional statistics in anyon collisions. *Science* **368**, 173–177 (2020).
30. Biswas, S. et al. Shot noise does not always provide the quasiparticle charge. *Nat. Phys.* **18**, 1476–1481 (2022).
31. Deviatov, E. V., Egorov, S. V., Biasiol, G. & Sorba, L. Quantum Hall Mach-Zehnder interferometer at fractional filling factors. *Europhys. Lett.* **100**, 67009 (2012).
32. Batra, N., Wei, Z., Vishveshwara, S. & Feldman, D. E. Anyonic Mach-Zehnder interferometer on a single edge of a two-dimensional electron gas. *Phys. Rev. B* **108**, L241302 (2023).
33. Bid, A., Ofek, N., Heiblum, M., Umansky, V. & Mahalu, D. Shot noise and charge at the 2/3 composite fractional quantum Hall state. *Phys. Rev. Lett.* **103**, 236802 (2009).
34. Biswas, S., Kundu, H. K., Umansky, V. & Heiblum, M. Electron pairing of interfering interface-based edge modes. *Phys. Rev. Lett.* **131**, 096302 (2023).
35. Choi, H. K. et al. Robust electron pairing in the integer quantum Hall effect regime. *Nat. Commun.* **6**, 7435 (2015).
36. Frigeri, G. A., Scherer, D. D. & Rosenow, B. Sub-periods and apparent pairing in integer quantum Hall interferometers. *Europhys. Lett.* **126**, 67007 (2019).
37. Kim, J. et al. Aharonov-Bohm interference in even-denominator fractional quantum Hall states. Preprint at https://arxiv.org/abs/2412.19886 (2024).
38. Moore, G. & Read, N. Nonabelions in the fractional quantum Hall effect. *Nucl. Phys. B* **360**, 362–396 (1991).

Methods

Sample fabrication process

The mesa of the device, which had dimensions 250 × 650 μm², was prepared in a GaAs/AlGaAs heterostructure (Supplementary Fig. 1) by wet etching in H_2O_2:H_3PO_4:H_2O = 1:1:50 for 100 s. The two-dimensional electron gas was 170 nm below the surface. Ohmic contacts were deposited at the edge of the mesa and within the mesa area (for testing the interface modes). The sequence of the evaporation by order of deposition was Ni (15 nm), Au (260 nm), Ge (130 nm), Ni (87.5 nm) and Au (15 nm). Contacts were annealed at 440 °C for 80 s. The sample was covered by 30 nm of insulating HfO_2, followed by evaporation of large metallic gates, Ti (5 nm) and Au (15 nm). The charged gates separated the device area into three regions with fillings ν_a, ν_b and ν_d. The mesa was covered by 25 nm of a HfO_2 layer, followed by a deposition of QPCs, a modulation gate and a small top gate in the middle of the bulk, with a radius of 0.5 μm (or 0.35 μm). In the final step, ohmic contacts, large metallic gates, the QPCs and the modulation gate were connected to large pads with thick gold lines. The top gate was connected by an air bridge and gold lines that passed over the HfO_2-coated metallic gates.

Data availability

The data that support the plots within this paper and other findings of this study are publicly available at https://doi.org/10.5281/zenodo.15395283 (ref. 39). Source data are provided with this paper.

39. Ghosh, B. Coherent bunching of anyons and their dissociation in interference experiments. *Zenodo* https://doi.org/10.5281/zenodo.15395283 (2025).

Acknowledgements M.H. thanks Y. Ronen for fruitful discussions. D.F.M. acknowledges many illuminating conversations on quantum Hall interferometry with Y. Ronen. B.G. thanks A. K. Paul for his helpful comment that improved the device. M.L. thanks the Ariane de Rothschild Women Doctoral Program for their support. D.F.M. acknowledges the support of the Israel Science Foundation (Grant No. 2572/21) and the Deutsche Forschungsgemeinschaft (DFG) within the CRC network TR 183 (Project Grant No. 277101999). M.H. acknowledges the support of the European Research Council under the European Union's Horizon 2020 research and innovation programme (Grant Agreement No. 833078) and the support of the Israel Science Foundation (Grant No. 1510/22).

Author contributions B.G. fabricated the devices. B.G. and M.L. performed the measurements and analysed the data with the input from M.H. M.H. supervised the design, execution and data analysis in the experiment. D.F.M. worked on the theoretical aspects and data analysis. V.U. grew the GaAs heterostructures. All authors contributed to the writing of the manuscript.

Competing interests The authors declare no competing interests.

Additional information
Supplementary information The online version contains supplementary material available at https://doi.org/10.1038/s41586-025-09143-3.
Correspondence and requests for materials should be addressed to Moty Heiblum.
Peer review information *Nature* thanks the anonymous reviewers for their contribution to the peer review of this work. Peer reviewer reports are available.